Microfluidic enrichment, isolation and characterization of disseminated melanoma cells from lymph node samples

Kathrin Weidele[1†], Nataša Stojanović[1†], Giancarlo Feliciello[1], Aleksandra Markiewicz[2], Sebastian Scheitler[1], Barbara Alberter[1], Philipp Renner[3], Sebastian Haferkamp[4], Christoph A. Klein [1,2] and Bernhard Polzer [1]

[1]Division of Personalized Tumour Therapy, Fraunhofer Institute for Toxicology and Experimental Medicine, 93053, Regensburg, Germany
[2]Experimental Medicine and Therapy Research, University of Regensburg, 93053, Regensburg, Germany
[3]Department of Surgery, University Medical Center, 93053, Regensburg, Germany
[4]Department of Dermatology, University Hospital Regensburg, 93053, Regensburg, Germany

For the first time in melanoma, novel therapies have recently shown efficacy in the adjuvant therapy setting, which makes companion diagnostics to guide treatment decisions a desideratum. Early spread of disseminated cancer cells (DCC) to sentinel lymph nodes (SLN) is indicative of poor prognosis in melanoma and early DCCs could therefore provide important information about the malignant seed. Here, we present a strategy for enrichment of DCCs from SLN suspensions using a microfluidic device (Parsortix™, Angle plc). This approach enables the detection and isolation of viable DCCs, followed by molecular analysis and identification of genetic changes. By optimizing the workflow, the established protocol allows a high recovery of DCC from melanoma patient-derived lymph node (LN) suspensions with harvest rates above 60%. We then assessed the integrity of the transcriptome and genome of individual, isolated DCCs. In LNs of melanoma patients, we detected the expression of melanoma-associated transcripts including *MLANA* (encoding for MelanA protein), analyzed the *BRAF* and *NRAS* mutational status and confirmed the malignant origin of isolated melanoma DCCs by comparative genomic hybridization. We demonstrate the feasibility of epitope-independent isolation of LN DCCs using Parsortix™ for subsequent molecular characterization of isolated single DCCs with ample application fields including the use for companion diagnostics or subsequent cellular studies in personalized medicine.

Introduction

The presence of disseminated cancer cells (DCCs) in lymph nodes (LNs) is a marker of metastatic spread and correlates with early recurrence and shortened survival in melanoma.[1–3] The sentinel lymph node (SLN), the first draining node to be involved in lymphatic spread, is usually the preferred site of early melanoma metastasis and already the detection of three or fewer cells per million leukocytes in the sentinel node was reported to affect the risk of death.[2] Since recent data indicate that some but not all stage III melanoma patients (i.e. those with LN involvement) benefit from BRAF-targeting[4] or immune checkpoint blockade,[5] the need to molecularly define early systemic cancer becomes evident. Early detection and molecular characterization of DCCs for therapy-relevant genetic changes could therefore become an important diagnostic and prognostic tool in assessing cancer progression and tumor staging, as well as influence clinical decisions for appropriate therapies and treatment plans.[6,7] In routine clinical pathology, the evaluation of resected LNs is conventionally performed by histopathology using a limited number of tissue

Tumor Markers and Signatures

What's new?
Early metastatic spread to sentinel lymph nodes provides important staging information for melanoma patients. In addition, adjuvant therapies are increasingly explored in node-positive patients, making the availability of companion diagnostics necessary. Thus, here the authors established a protocol for the analysis of single disseminated cancer cells (DCCs) from lymph nodes applying a commercially available epitope-independent microfluidic enrichment method. They show that cell suspension from lymph nodes can be processed and that microfluidics-enriched cells are viable and amenable for subsequent molecular analysis. The presented workflow represents a novel tool for in-depth characterization of lymph node-derived cancer cells, including early metastasis precursors.

sections.[8] As only a minor proportion of the LN is examined, the occurrence of individual DCC and therefore tumor burden may be underestimated.[9] However, less extensive and more precise techniques are needed. We recently showed that the quantitative analysis of DCCs from disaggregated LN enables an accurate evaluation of the metastatic spread.[2,10,11] While this approach allows analysis of the entire LN and not only selected sections, the time-consuming screening step of millions of lymph node cells remains a limitation. Automation, especially in combination with better DCC enrichment strategies, would strongly enhance applicability in diagnostic workflows. Concurrently, the detection, quantification and molecular analysis of DCCs represents an important tool for understanding the biology of the metastatic process and may in the future aid in therapy decisions. Consequently, technical approaches that enable isolation of DCCs with increased purity and viability are prerequisite for subsequent comprehensive analyses.

Recent publications demonstrated that the Parsortix™ device, a size-based system utilizing microfluidic technology, is capable of capturing cells spiked in blood of healthy donors or circulating tumor cells (CTCs) from blood samples of cancer patients.[12–15] Independent of surface markers, tumor cells can be captured according to their size and deformability, allowing the enrichment of heterogeneous cancer cells. Apart from classical histology or immunohistochemical methods, where cells need to be fixed, Parsortix™ system releases viable cells offering a broader range of molecular analysis or functional testing. We adapted this system for DCC detection and isolation from disaggregated LN tissue. This workflow enables, on the one hand, an automated enrichment and quantitative measurement of tumor cells from LN cell suspensions and, on the other hand, the opportunity for molecular characterization of the enriched cell population. By optimizing the system for handling LN cell suspensions, we tested up to 10 million LN cells, which could be processed within 2 hr including capture on the cassette and harvest, rendering this approach attractive for clinical research.

In our study, we tested the functionality and application of a microfluidic-based enrichment technology and developed a workflow enabling harvesting and characterization, thus monitoring of DCC in LN cell suspensions. We also investigated if enriched cells are viable and therefore suited for *in vitro* culture or subsequent molecular downstream single-cell analysis on transcriptome and genome levels opening new opportunities for translational research.

Materials and Methods
Cell lines
The human melanoma cell line MelHo (obtained from DMSZ), lung cancer cell line A549 (from ATCC) and breast cancer cell line SKBR3 (from DMSZ) were used to test functionality and application of the Parsortix™ technology (ANGLE plc, Guildford, UK). Authentication and identity of all cell lines were tested by DNA fingerprinting using Cell ID™ system from Promega before experimental use. Cell lines were cultivated in RPMI 1640 (MelHo) or DMEM (SKBR3, A549) supplemented with 10% fetal bovine serum, penicillin (100 units/ml), streptomycin (100 μg/ml; all from PAN-Biotech) and 1x GlutaMAX (Life Technologies) at 37°C in 5% CO_2.

EDTA blood collection and gradient centrifugation
In initial experiments, 60% Percoll (GE Healthcare) gradient enriched blood samples were used as a model for LN samples.[10] For spiking experiments, blood was drawn from healthy volunteers after obtaining informed written consent and collected in BD Vacutainer™ blood collection tubes with K2EDTA (BD).

Quantitative cell spiking
Cell lines were prelabeled with fluorescent dye DiI according to manufacturer's protocol (Promokine). For each experiment, 200 labeled cells were spiked in 4 ml blood of healthy volunteers, the Percoll enriched interphase or 4 million LN cells for subsequent microfluidic enrichment. To estimate the size and number of cells spiked, the same amount of labeled cells were spiked in PBS at least in triplicates in 48 well plates and microscopically analyzed as internal controls. The mean value of the counted cells was defined as number of spiked cells and used for the calculation of capture and harvest rates.

Patient LN samples
For our studies, we obtained LN tissue from sentinel node biopsies and radical lymphadenectomies. All patients provided written informed consent before surgery and the study was approved by the University of Regensburg Ethics Committee (ethics vote 07-079). Single-cell suspensions of LN samples were prepared as previously described[10] and filtrated with a 100 μm cell strainer. Cells were resuspended in a total volume of 100 μl PBS/2% FCS and stained with anti-MCSP-PE antibody (clone EP-1 from Miltenyi Biotec, Germany) for 20 min

as recommended by the manufacturer. An equivalent of 200 MCSP-stained cells was adjusted to a volume of 4 ml in PBS/2% FCS for subsequent enrichment.

Cell separation by Parsortix™ technology

Blood samples were processed using the Parsortix™ system (Angle plc, Guildford, UK) as recommended by the manufacturer. Briefly, 10 μm or 6.5 μm cassettes were primed shortly before blood separation with PBS. For processing interphase or LN samples, cassettes were primed with buffers containing either BSA (2% or 5%) alone or a combination EDTA (2 mM) with 0.5% BSA. In the first step, cells were enriched based on their size and deformability (capture) and collected in the second step (harvest) in a well of a 48 well plate. Subsequently, the number of labeled cells in the cassette before harvesting and the number of harvested cells were determined and normalized to control counts, enabling the calculation of capture and harvest rates as follows:

Capture rate = (number of captured cells on the cassette/ number of spiked cells) × 100.

Harvest rate = (number of harvested cells/number of spiked cells) × 100.

Cells detected in the cassette after harvest were named 'Remained cells'. Theoretically, the sum of harvested and remained fraction of cells should be equal to the number of captured cells. However, 100% recovery in practice is not possible because of minor cell loss within the tubing of the system. Detection and imaging of captured, harvested and cultured cells were performed using a fluorescence microscope (Olympus) or light microscope (Leica). Cell size was measured with cellSens Olympus software. For *in vitro* culture experiments, cells were collected after harvest in complete culture medium and cultivated for indicated time points.

Single-cell isolation and molecular amplification

After harvest, cells were collected and transferred on chamber slides (Nunc, Thermo Fisher Scientific, Waltham, MA), enabling manual isolation of single cells and cell pools using a micromanipulator (Eppendorf). For further molecular downstream analysis, isolated single cells were subjected to simultaneous whole transcriptome amplification (WTA) and whole genome amplification (WGA) as previously described.[16–18] Quality of WGA and WTA products was assessed using multiplex PCR assays (*Ampli*1™ QC Kit and *Ampli*1™ WTA QC Kit, Menarini Silicon Biosystems, Bologna, Italy).

Detection of expression of melanoma-associated markers using endpoint PCR

WTA products with good quality (>1 quality control transcripts positive) were tested for the expression of melanoma-associated transcripts *PMEL* (gp100), *MLANA* (MelanA), *S100B* and *DCT* (TRP2). *PTPRC* (CD45) expression was used for identification of nonmelanoma cells. Following primer pairs (final concentration 0.5 μM) were used (5′ to 3′): *PTPRC* forward TTAGGGAC

ACGGCTGACTTC and reverse GCTTTGCCCTGTCACAAA TA; *PMEL* forward CCTCTTGCTCATTCCAGCTC and reverse TCCAAAGTCCCAGGTGTAGG; *MLANA* forward GCTCATCGGCTGTTGGTATT and reverse ATAAGCAGG TGGAGCATTGG; *S100B* forward ATTCTGGAAGGGAGGG AGAC and reverse CGTGGCAGGCAGTAGTAACC; *DCT* forward CCAGCTGGGAAACTGTCTGT and reverse AACCC TTCCAAAGCATTCC.

BRAF and NRAS sequencing

Mutations in *BRAF* and *NRAS* genes were assessed in single cells and pools from WGA products with good quality (genome integrity index; GII: >2 quality control PCR-fragment positive).[19] The used primer pairs cover *BRAF* exon15 (encompassing mutations in codon 600), *NRAS* exon2 and *NRAS* exon3 (encompassing mutations in codon 12–13 and 61, respectively). Following primer pairs (final concentration 0.5 μM) were used (5′ to 3′): *BRAF* forward CTCTTCATAATGCTTGCTCTG and reverse TCCAGACAACTGTTCAAACTG; *NRAS* exon2 forward GGTTTCCAACAGGTTCTTGC and reverse TCCGA CAAGTGAGAGACAGG; *NRAS* exon3 forward CCCCTT ACCCTCCACACC and reverse CCGCAAATGACTTGCTAT TATTG. PCR products were purified with PCR purification kit (Qiagen) and sequenced using Sanger sequencing by a commercial provider (Sequiserve).

Microarray-based comparative genomic hybridization

Copy number alterations (CNAs) were analyzed by array comparative genomic hybridization (aCGH) in four DCCs isolated from two melanoma patients (patient 1 and patient 3). Briefly, WGA products were labeled by PCR-based labeling using incorporation of dye-conjugated dNTPs, hybridized on oligonucleotide-based slides SurePrint G3 Human CGH 4x180K (Agilent Technologies) and analyzed as published earlier.[20] Aberrant regions were recognized using ADM-2 algorithm with threshold set to 8.0. The centralization parameters were set to a threshold of 6.0 and bin size of 10. The aberration filter applied to avoid false-positive calls was the log2 ratio of 0.3 and the minimum number of probes in the aberrant interval was set to 200. All data have been deposited in NCBIs Gene Expression Omnibus (GEO, http://www.ncbi.nlm.nih.gov/geo/) and assigned series accession number GSE118478.

Statistical analysis

When not stated otherwise, experiments were done at least in triplicates and are shown as a median value. Statistical significances were calculated using Mann–Whitney test with GraphPad Prism Software (version 5).

Results

Identification of the optimal microfluidic cartridge for tumor cell enrichment

One major advantage of a microfluidic platform is the epitope-independent separation of CTCs from the rest of blood cell
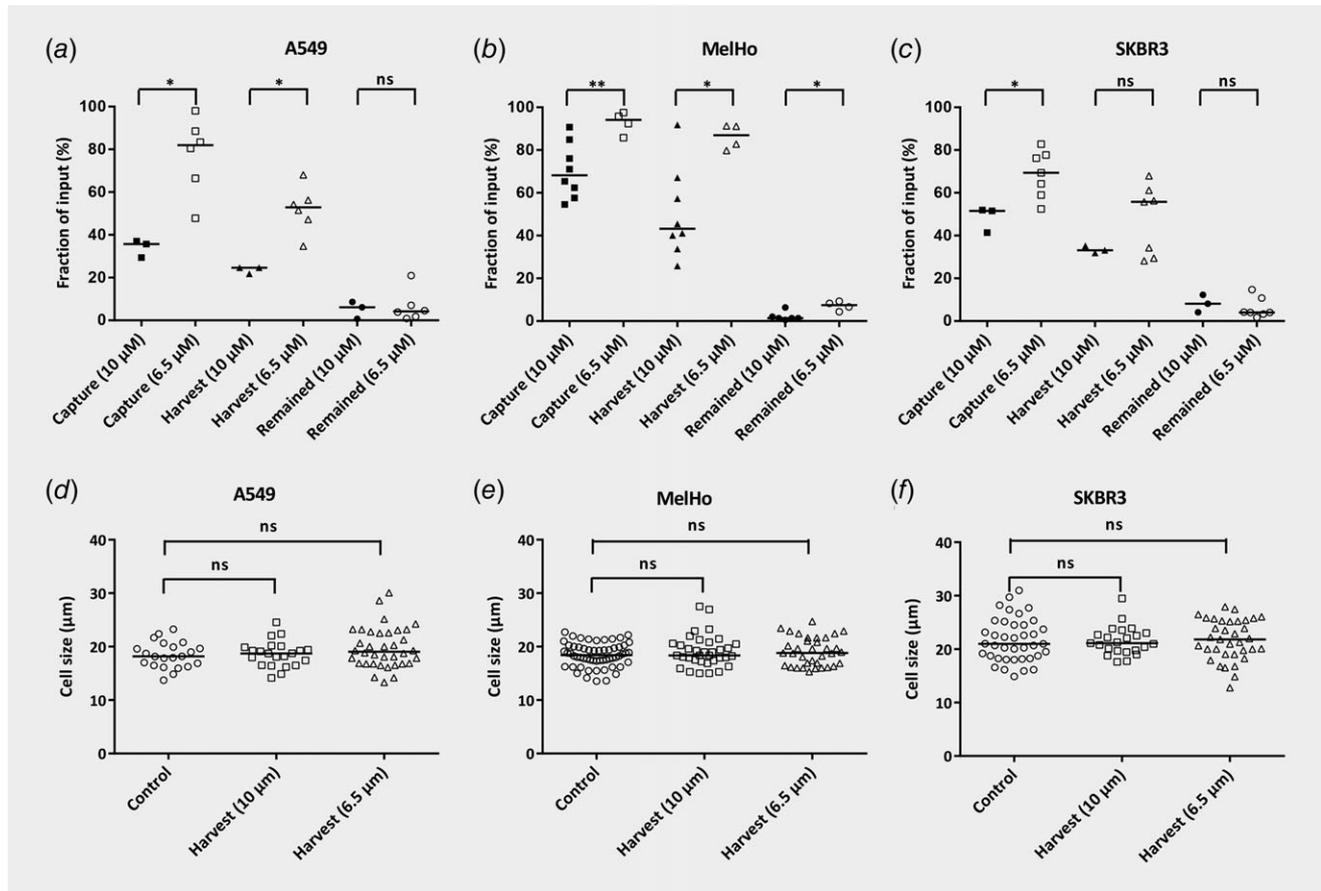
Figure 1. Comparison of **6.5** *vs.* **10** μm cassettes. (*a–c*) A549 (*a*), MelHo (*b*) and SKBR3 (*c*) cells were spiked into blood of healthy donors and samples were processed on Parsortix™ system. Each sample was analyzed on two different cassettes (**6.5** *vs.* **10** μm gap size). The fraction of captured cells, harvested cells and cells that remained in the cassettes are shown as percentages of the input on the y axes. (*d–f*) Cell size distribution, before (control) and after processing through the cassette (harvest), is shown for the cell lines A549, MelHo and SKBR3 and respectively. Horizontal lines on dot-plots represent median (*p* ‹ **0.05**; **p* ‹ **0.01**; Mann–Whitney *U*-test).

populations. For this purpose, two types of microfluidic cassettes were designed by the manufacturer. The cassettes differ according to the size of the terminal gap through which most of the blood cells flow through, while tumor cells remain captured within the stairway-like structure of the cassette. In order to optimize the workflow for the processing of LN suspensions, we compared the numbers of captured and harvested (for definitions, see Materials and Methods section) cells between the cassette types. For this purpose, we performed spiking experiments with three different cell lines: MelHo, SKBR3 and A549. For each experiment, we spiked 200 prelabeled cells in 4 ml of blood and performed cell separation on the device. We found that 6.5 μm cassettes have higher capture and harvest rates compared to 10 μm cassettes for all three cell lines tested (Figs. 1*a*–1*c*). The median harvest rate was normalized to the number of spiked in cells (input) and for 10 μm cassette ranges from 24.6% (A549) to 43.23% (MelHo), while the median harvest rate for 6.5 μm cassette ranges from 52.86% (A549) to 86.95% (MelHo). Therefore, 6.5 μm cassettes were significantly better (capture rates: MelHo - $p = 0.0081$, A549 - $p = 0.0238$ and SKBR3 - $p = 0.0167$;

harvest rates: MelHo - $p = 0.0485$, A549 - $p = 0.0275$ and SKBR3 - $p = 0.5167$) and were used for further experiments.

Next, we investigated if size-defined subpopulations of tumor cells were selected during processing of the sample on Parsortix™ device. The diameter of tested cell models in suspension was approximately 18 μm (MelHo, range 13.56–22.72 μm and A549, range 13.71–23.26 μm) and 21 μm (SKBR3 range 14.89–30.99 μm). We compared tumor cells diameters before separation and after harvesting on both cassette types (Figs. 1*d*–1*f*) and found the same distribution of cell diameters. This indicates low contribution of size-based selection within the tumor cell population.

Tumor cells enriched with Parsortix™ device are viable and suitable for molecular analyses

To analyze if the enrichment workflow influences cell viability, DNA and RNA quality, melanoma cancer cells (MelHo) were spiked into the blood of a healthy donor, processed on Parsortix™ system, harvested and manually isolated from suspension using a micromanipulator. To assess the DNA quality
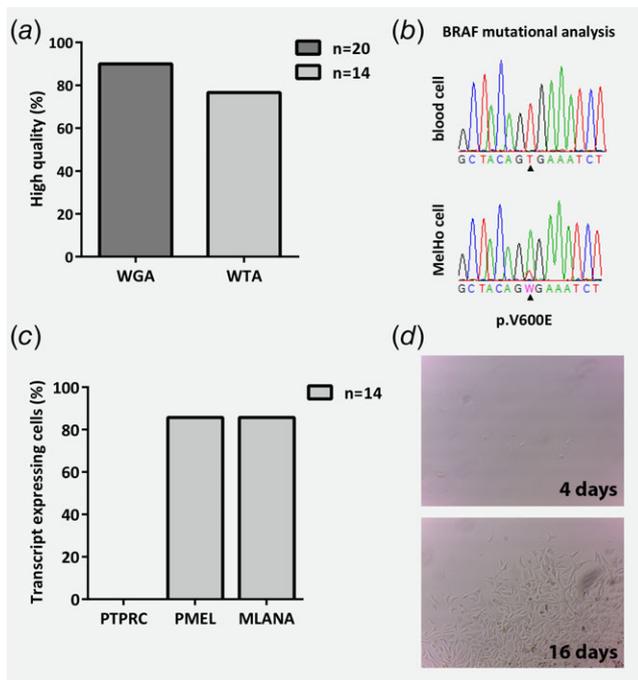
Figure 2. Isolation of single MelHo cells, molecular analysis and *in vitro* propagation. (*a*) Quality of WGA and WTA products of MelHo cells isolated after spike in experiments as determined by Ampli1™ WGA QC and WTA QC, respectively. (*b*) Sanger sequencing confirms presence of *BRAF^V600E* mutation characteristic for MelHo cells but not for blood cells from healthy donors. (*c*) Transcriptomes of all analyzed MelHo cells (*n* = 13) contained *PMEL* (gp100) and *MLANA* (Melan-A) transcripts and were negative for *PTPRC* transcript (CD45). (*d*) Photomicrographs of MelHo cells cultured *in vitro* for 4 and 16 days after recovery from Parsortix™ cassette.

of the processed cells, we performed single cells WGA and applied an informative multiplex PCR-assay that was previously shown to reflect the integrity of the genomic DNA by the number of bands obtained from a single cell.[19] We could show that 90% of the analyzed single cells (*n* = 20) retained high DNA quality (Fig. 2*a*) as represented by genomic integrity index (GII; Supporting Information Fig. S1A). Cells with high DNA quality (GII >2) were then selected for further analysis of *BRAF* mutation status and the p.V600E mutation, characteristic for MelHo cell line, was detected in 5/5 cells (Fig. 2*b*).

To assess RNA integrity, we isolated mRNA from single cells and performed single cell WTA as reported.[21] The amplified cDNA library was of a high quality determined from the number of bands obtained in a multiplex PCR, WTA-QC (Fig. 2*a*). Out of all analyzed single cells, 85.7% (12/14) showed at least two bands in a multiplex PCR assay (Supporting Information Fig. S1B). When we analyzed the 12 single cells with >1 PCR band in the QC-assay and detected the melanoma-specific transcripts *PMEL* (coding for gp100 protein) and *MLANA* (coding for MelanA protein) in all analyzed single cells (Fig. 2*c*). None of the analyzed single cells expressed the *PTPRC* transcript, (coding for the CD45 antigen) characteristic for white blood cells.

As a proof of concept whether the tumor cells in the microfluidic device remain viable, we tested if they can be propagated in culture. For this purpose, we spiked 200 prelabeled MelHo cells in 4 ml of blood and performed cell separation on the device. The harvest was collected and starting from 169 cells MelHo cells repopulated the whole 6 cm culture dish within 16 days (Fig. 2*d*).

Priming of microfluidic cassettes enables processing of LN cell suspensions

LNs are routinely excised and contain higher numbers of tumor cells than blood in early, nonmetastatic disease stages. Therefore, we explored the potential of the Parsortix™ device for automated enrichment of DCCs found in LN of cancer patients. We first processed LN cell suspension from melanoma patient with high number of DCCs, which were positive for melanoma markers and labeled with fluorescent antibody for melanoma marker MCSP. By using standard separation protocol for the Parsortix™ device with PBS cassette priming, we successfully captured tumor cells (Fig. 3*a*) but were unable to harvest the cells that remained stuck within the cassette (Fig. 3*b*). We suspected that preparation of LN suspension[10] might increase the stickiness of the cells. To overcome this problem, we tested different protocols for cassette priming.

Different protocols were first tested using blood samples spiked with A549 or MelHo cells. We used blood (4 ml) from healthy donors, processed it on 60% Percoll density gradient medium and isolated interphase peripheral blood lymphocytes in which we spiked in fluorescently labeled A549 cells. To provide optimal distribution of the cells after gradient enrichment, we processed a total volume of 15 ml in parallel on two devices with a PBS-primed cassette or a cassette primed with 5% BSA. As shown in Figure 3*c*, priming the cassette with 5% BSA significantly increased capture and harvest rates up to 63% for 6.5 μm cassette and up to 30% for MelHo when using 10 μm cassettes (Supporting Information Figure S2). However, as a downside, we experienced that high BSA concentration is not compatible with long-term usage of the microfluidic platform because of frequent blockage of the system by crystallized BSA. Therefore, we reduced the BSA concentration to 2% and compared it with an alternative priming solution, containing 2 mM EDTA +0.5% BSA in order to reduce cell adherence. Interestingly, both protocols successfully prevented system blockage and generated similar capture and harvest rates (Fig. 3*d*).

With these new priming protocols, we then spiked fluorescently labeled MelHo cells in 4 million cells from LN of healthy donors or unstained SLN from cancer patients. We applied two different protocols – cassette priming with 2 mM EDTA + 0.5% BSA or cassette priming with 2% BSA. As shown in Figure 4*a*, there was no difference in capture and harvest rates between the two procedures. In addition, 70–80% of cells had high WGA (*n* = 10) and 87–100% of cells (*n* = 8) had high WTA quality, with no difference between the two protocols (Figs. 4*b* and 4*c*).
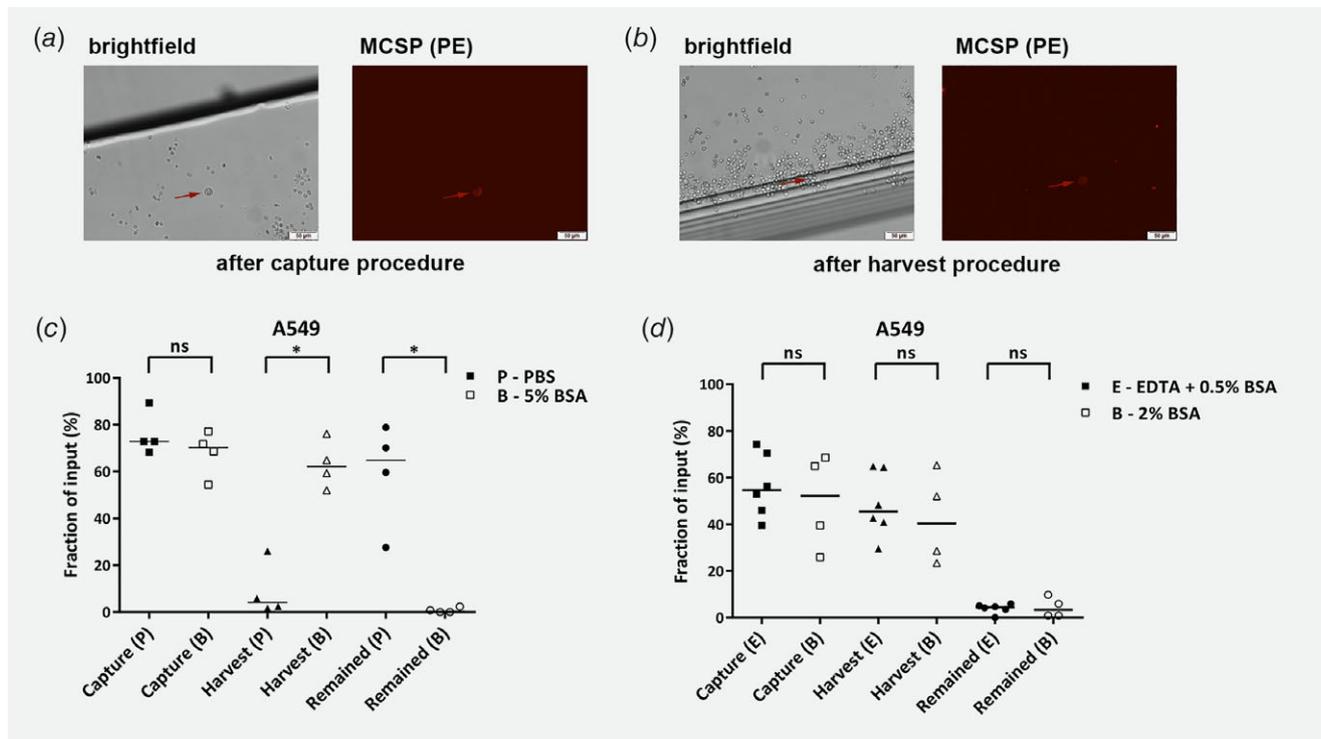
Figure 3. Processing of lymph node samples on Parsortix™ system. (*a* and *b*) Lymph node suspension with high DCC number was prestained for MCSP and processed on Parsortix™ device. Cassette was primed with PBS before loading the sample. Photomicrographs of a cassette after separation (*a*) and harvest procedure (*b*) are shown. Red arrows indicate possible melanoma cells that are retained in the cassette even after harvest procedure (scale bar - **50** μm). (*c* and *d*) Prestained A**549** cells were spiked into the interphase of blood from healthy donors which was processed on **60**% Percoll. **6.5** μm cassettes were primed with PBS only or with **5**% BSA diluted in PBS (*c*). **6.5** μm cassettes were primed with **2** mM EDTA +**0.5**% BSA or with **2**% BSA only (*d*). The fraction of captured cells, harvested cells, and cells that remained in the cassettes are shown as percentages of the input on the y axes. Horizontal lines on dot-plots represent median (*$*p < 0.05$; $**p < 0.01$; ns,no statistical significance; Mann–Whitney *U*-test).

Finally, we processed three LN samples of melanoma patients containing high numbers of DCCs to enable experimental comparisons. The samples were stained against the melanoma marker MCSP (Fig. 4*d*) and brought to a dilution of 200 MCSP-positive cells per sample. With both priming procedures, capture and harvest rates were similar and relatively high with, on average, 72.8% of the cells being recovered (Fig. 4*e*). From two LN samples (patient 1 and patient 3), we isolated 30 single cells and assessed DNA and RNA quality, defined as <1 band in each multiplex QC-PCR-assay, in order to perform combined genome and transcriptome analysis of same cells. From one patient (patient 2), due to technical reasons, we could isolate only RNA, not DNA, from 19 cells. The difference in DNA and RNA quality between cells processed with two priming protocols was negligible. Specifically, 60–73.3% of DCCs isolated from patients' LNs after both priming protocols had high DNA quality and 76–77.2% had high RNA quality (Figs. 4*f* and 4*g*, respectively).

Molecular analysis of isolated DCCs confirms melanoma origin

The isolated single cells of the three melanoma patients (for clinical data of patients, see Fig. 5*a*) were then subjected to

molecular analysis. The general workflow enabling enrichment and characterization of DCCs from patient LN samples is highlighted in Figure 5*b*. To confirm melanoma origin, 38 single cells from the previous experiment with high mRNA quality of the three patients were analyzed for presence of melanoma transcripts. All but three cells (92%) expressed at least one melanoma-associated transcript. The fraction of cells positive for the melanoma transcripts tested varied and *MLANA* transcript was most frequently detected (Fig. 5*c*). To further confirm that the isolated cells were indeed cancer cells, we performed mutational analysis of 13 single cells and 4 cell pools by Sanger sequencing (representative pictures are shown in Fig. 5*d*). In one patient (patient 1), all nine analyzed DCCs and two cell pools carried a hot spot mutation in exon 2 of *NRAS* at position G12C. In the second patient (patient 3), four analyzed single cells and two cell pools carried the *BRAF* hot spot mutation V600E. Because of unsuccessful DNA isolation due to technical reasons, we could not perform mutational analysis of the cells from patient 2 (summarized data of all three melanoma patients in Supporting Information Table S1).

To demonstrate whole genome coverage and prove the melanoma origin of the isolated cells, we performed aCGH on four single cells isolated from two patients (two cells from patient
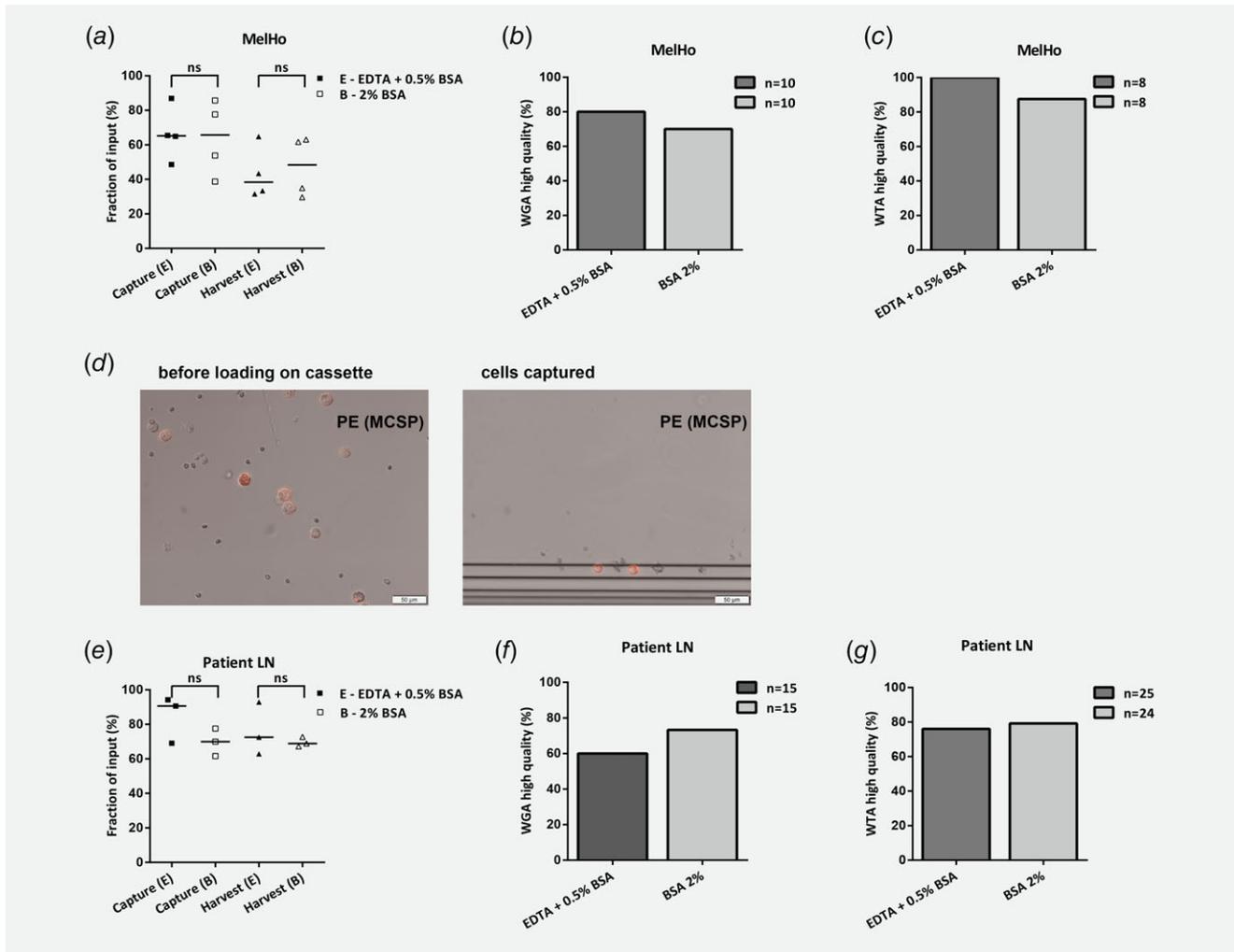
Figure 4. Validation of LN processing protocol with MelHo cell line and patient samples. (*a*) MelHo cells were spiked into the LN suspension of healthy donors or cancer patients and samples were processed on Parsortix™ system. Cassettes were primed with **2 mM EDTA +0.5**% BSA or 2% BSA only and the fraction of captured and harvested cells are shown as percentages of the input on the y axes, horizontal lines on dot-plots represent median (ns, no statistical significance; Mann–Whitney *U* test). (*b* and *c*) Harvested single MelHo cells were isolated by micromanipulator and the percentage of cells with high quality WGA (*b*) and WTA (*c*) is shown (*N* refers to the total number of analyzed cells). (*d*) Disaggregated LN tissue from melanoma patients after lymphadenectomy and high tumor cell load were stained for MCSP, diluted to a total of **200** positive cells and loaded on the cassette. Photomicrographs show an example of patients MCSP stained cells before loading on Parsortix™ system and captured in the cassette. (*e*) No difference between priming with **2 mM EDTA +0.5**% BSA or 2% BSA only could be observed (ns, no statistical significance; Mann–Whitney *U* test). (*f* and *g*) Harvested single melanoma cells were isolated by micromanipulator and the percentage of cells with high quality WGA (*f*) and WTA (*g*) is shown (*N* refers to the total number of analyzed cells).

1 and two cells from patient 3). The presence of genomic aberrations confirmed again their malignant origin and, importantly, revealed that the cells harbor genomic alteration characteristic of melanoma, such as 7q or 8q amplification and CDKN2A deletion on 9p21.3. Additionally, sibling cells from the same patient shared some common aberration marking their clonal origin but they displayed heterogeneous CNAs (Fig. 5*e*).

Discussion

In our study, we developed a workflow enabling enrichment, detection, isolation and molecular characterization of DCCs from LN suspensions of melanoma patients by using a marker-free

microfluidic-based technology. The protocol comprises a reliable workflow to isolate viable DCCs with high DNA and RNA quality, which allows detailed molecular characterization and the potential to propagate viable patient-derived cells for clinical and preclinical studies in cell culture.

It was previously shown[12–14] that the Parsortix™ system enables efficient capture and harvest of spiked tumor cells from peripheral blood samples from a variety of tumor types when using cassettes with 10 μm gap size. Recently, better recovery rates were also reported for MCF7 cells[22] using 6.5 μm cassettes. We directly compared the capture and harvest rates of cassettes with 10 μm *vs.* 6.5 μm gap size and
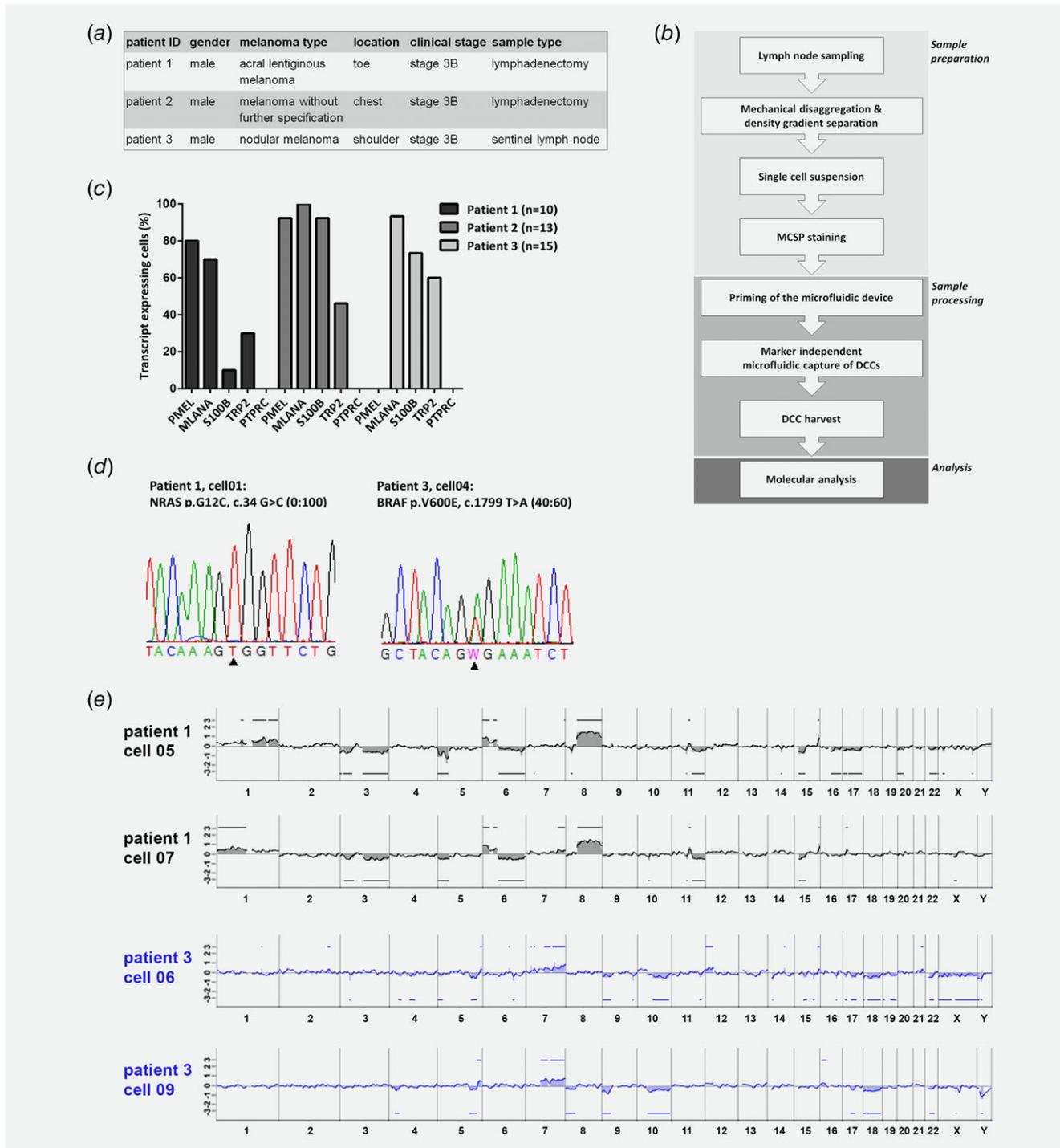
Tumor Markers and Signatures

Figure 5. Molecular analysis of DCCs from LNs of melanoma patients. (*a*) Clinical data of the three melanoma patients. (*b*) Workflow for DCC enrichment of melanoma LN samples. (*c*) Transcriptomes of all analyzed DCCs from patient **1, 2** and **3** (*n* = 10; 13; 15, respectively) were negative for *PTPRC* transcript (CD**45**). **92.1**% of cells were positive for at least one or more transcripts characteristic for melanoma cells (*PMEL, MLANA, S100B, TRP2*). (*d*) Sanger sequencing confirms presence of *NRAS*^{G12C} in cells isolated from patient **1** as well as *BRAF*^{V600E} mutation from patient **3**. (*e*) aCGH genome view of the analyzed DCCs for patient **1** and patient **3** that validates the presence of typical melanoma genomic aberrations and the malignant origin of the isolated cells.

observed significantly improved overall recovery of target cells using the smaller gap size. Independently of the cassette type, cell diameter distribution was the same before and after harvest, indicating that no size-defined subpopulation of the cells was selected during the enrichment procedure. This result suggest that deformability plays a more important role

in tumor cell enrichment than cell size, at least for the cell lines tested (MelHo, A549, SkBr3). As a drawback, we also noticed the retention of more red blood cells within 6.5 μm cassettes and sevenfold higher leukocyte contamination after harvest. However, total cell numbers after harvest are still in a range that does not significantly inflict cell isolation procedures for subsequent analysis.

The established workflow is compatible with different methods for molecular and functional analysis. We could show, that the majority of isolated cell line cells result in samples of high DNA and RNA quality after single cell whole genome or transcriptome amplification by *Ampli*1™ technologies. Hence, the workflow can be used for downstream applications as gene expression profiling, mutational analysis or genome-wide copy number profiling of single cells or cell pools.[17,23] Moreover, in contrast to other tumor cell enrichment technologies, where cells need to be fixed (CellSearch®) or captured on a membrane after microfiltration (ISET®, MetaCell®, ScreenCell®), cells processed on Parsortix ™ can be easily released, are viable and suited for *in vitro* culture. The developed protocol can be applied on patients' samples, which enables the establishment of DCC-derived *in vitro* models for functional studies.

We next asked the question, if we could transfer the technology and workflow developed for blood-based analysis of CTCs to other patient-derived samples, particularly for DCC detection and isolation from disaggregated LN samples, which holds great promise for improving LN staging.[2,7] Assessment of cancer spread to LNs is part of the TNM staging system in most cancers; however, routine histopathological analysis is associated with limitations in sensitivity and restricted to the presence or absence, but does not allow quantitative enumeration of DCCs.[24,25] By contrast, in a recent study, we could show that the quantitative analysis of lymphatic cancer cell dissemination on the single-cell level is superior to classical histopathology.[2,10] Moreover, molecular signatures derived from single DCCs were shown to predict LN colonization and patient survival,[7] highlighting the need for more profound analysis of DCCs. Therefore, combining quantitative detection of cancer cells in disaggregated LNs and superior tumor cell enrichment by microfluidic-based cell separation has a great potential, as (i) tumor cells are homogenously distributed within the cell suspension, (ii) the work load is reduced and (iii) a broader range of patient material can be analyzed providing a concentrated sample of viable cells for sophisticated molecular or functional assays.

Although initial experiments using LN samples with high numbers of DCCs showed successful separation within the cassette, it was not possible to harvest the target cells. For currently unknown reasons, tumor cells got stuck in the device and could not be eluted. Possibly, the Percoll density gradient medium, containing colloidal silica particles coated with polyvinylpyrrolidone, caused higher adherence of the cassette and cell surface. Another explanation might be that serum proteins

(i.e., albumin), which could smoothen the surface of the microfluidic cassette during the processing of blood samples, are lacking in LN samples. To overcome this problem, we tested different protocols for cassette priming and added BSA or EDTA to prevent cell adherence as also experienced by Xu *et al.*[12] Unfortunately, although showing very good performance, high concentration of BSA (5% solution in PBS buffer) crystallized within the microfluidic device and thus we recommend the usage of lower BSA concentration with or without EDTA (we tested 2% BSA and 0.5% BSA plus 2 mM EDTA). Both coating solutions resulted in comparable harvest rates of MelHo cells spiked in LN samples (harvest rates >40%). During protocol establishment, we processed up to 10 million LN cells, which were prediluted with PBS/2% FCS in a concentration of maximum $1 \times 10^6/2$ ml. The device has the potential to process even higher number of the cells but in order to avoid clogging and premature termination, the method has to be further optimized. In addition, a modification of the currently available cassettes may lead to improvement.

To validate our results and as a proof of concept we finally applied the workflow on LN suspensions from three melanoma patients. We observed a high recovery of MCSP-labeled DCC with harvest rates of more than 60%. Moreover, we confirmed the suitability of isolated cells for downstream analysis and proved the malignant origin of the isolated cells. High-quality cDNA (>76%) samples allowed targeted gene expression profiling of three patients, showing transcript expression of four selected melanoma marker (*MLANA, PMEL, S100B, DCT*). Interestingly, *MLANA* transcript was detectable in all three patients and expressed in the majority of the tested cells, whereas one patient was completely negative for *PMEL* expressing cells, highlighting the ability to collect and isolate different subpopulations of DCCs. In addition, high-quality DNA samples (>60%) of two patients resulted in the detection of melanoma-associated mutations in *BRAF* and *NRAS* gene and enabled detection of aberrant genomic profiles typical for melanoma.

In perspective, the implementation of the presented workflow represents a novel tool for in-depth characterization of LN-derived cancer cells, including early metastasis precursors. Potential applications include development of companion diagnostics not only for melanoma, but also for DCCs of other LN-seeding cancer types. As the approach also allows isolation of viable cells, future studies may exploit the possibility for propagation of patient-derived cell models for preclinical and clinical studies in personalized medicine. The study is designed as a proof of principle to show new application of microfluidic devices in a detection and isolation of DCCs. However, new studies on LNs from several tumor entities, with higher number of samples, are ongoing.

Tumor Markers and Signatures

References

1. Scheri RP, Essner R, Turner RR, et al. Isolated tumor cells in the sentinel node affect long-term prognosis of patients with melanoma. *Ann Surg Oncol* 2007;14:2861–6.
2. Ulmer A, Dietz K, Hodak I, et al. Quantitative measurement of melanoma spread in sentinel lymph nodes and survival. *PLoS Med* 2014;11: e1001604.
3. Morton DL, Thompson JF, Cochran AJ, et al. Sentinel-node biopsy or nodal observation in melanoma. *N Engl J Med* 2006;355:1307–17.
4. Long GV, Hauschild A, Santinami M, et al. Adjuvant Dabrafenib plus Trametinib in stage III BRAF-mutated melanoma. *N Engl J Med* 2017; 377:1813–23.
5. Weber J, Mandala M, Del Vecchio M, et al. Adjuvant nivolumab versus ipilimumab in resected stage III or IV melanoma. *N Engl J Med* 2017;377: 1824–35.
6. Balch CM, Gershenwald JE, Soong SJ, et al. Final version of 2009 AJCC melanoma staging and classification. *J Clin Oncol* 2009;27:6199–206.
7. Werner-Klein M, Scheitler S, Hoffmann M, et al. Genetic alterations driving metastatic colony formation are acquired outside of the primary tumour in melanoma. *Nat Commun* 2018; 9:595.
8. Murali R, DeSilva C, McCarthy SW, et al. Sentinel lymph nodes containing very small (<0.1 mm) deposits of metastatic melanoma cannot be safely regarded as tumor-negative. *Ann Surg Oncol* 2012;19:1089–99.
9. Baisden BL, Askin FB, Lange JR, et al. HMB-45 immunohistochemical staining of sentinel lymph nodes: a specific method for enhancing detection of micrometastases in patients with melanoma. *Am J Surg Pathol* 2000;24:1140–6.
10. Ulmer A, Fischer JR, Schanz S, et al. Detection of melanoma cells displaying multiple genomic changes in histopathologically negative sentinel lymph nodes. *Clin Cancer Res* 2005;11:5425–32.
11. Ulmer A, Dietz K, Werner-Klein M, et al. The sentinel lymph node spread determines quantitatively melanoma seeding to non-sentinel lymph nodes and survival. *Eur J Cancer* 2018;91:1–10.
12. Xu L, Mao X, Imrali A, et al. Optimization and evaluation of a novel size based circulating tumor cell isolation system. *PLoS One* 2015;10:e0138032.
13. Hvichia GE, Parveen Z, Wagner C, et al. A novel microfluidic platform for size and deformability based separation and the subsequent molecular characterization of viable circulating tumor cells. *Int J Cancer* 2016;138:2894–904.
14. Chudziak J, Burt DJ, Mohan S, et al. Clinical evaluation of a novel microfluidic device for epitope-independent enrichment of circulating tumour cells in patients with small cell lung cancer. *Analyst* 2016;141:669–78.
15. Gorges TM, Kuske A, Rock K, et al. Accession of tumor heterogeneity by multiplex Transcriptome profiling of single circulating tumor cells. *Clin Chem* 2016;62:1504–15.
16. Klein CA, Schmidt-Kittler O, Schardt JA, et al. Comparative genomic hybridization, loss of heterozygosity, and DNA sequence analysis of single cells. *Proc Natl Acad Sci U S A* 1999;96:4494–9.
17. Klein CA, Blankenstein TJ, Schmidt-Kittler O, et al. Genetic heterogeneity of single disseminated tumour cells in minimal residual cancer. *Lancet* 2002;360:683–9.
18. Guzvic M, Braun B, Ganzer R, et al. Combined genome and transcriptome analysis of single disseminated cancer cells from bone marrow of prostate cancer patients reveals unexpected transcriptomes. *Cancer Res* 2014;74:7383–94.
19. Polzer B, Medoro G, Pasch S, et al. Molecular profiling of single circulating tumor cells with diagnostic intention. *EMBO Mol Med* 2014;6:1371–86.
20. Czyz ZT, Hoffmann M, Schlimok G, et al. Reliable single cell array CGH for clinical samples. *PLoS One* 2014;9:e85907.
21. Ulmer A, Stodulski M, Kohlhepp SV, et al. Iodine (III)-catalyzed rearrangements of imides: a versatile route to alpha,alpha-dialkylated alpha-hydroxy carboxylamides. *Chemistry* 2015;21:1444–8.
22. Lampignano R, Yang L, Neumann MHD, et al. A novel workflow to enrich and isolate patient-matched EpCAM(high) and EpCAM(low/negative) CTCs enables the comparative characterization of the PIK3CA status in metastatic breast cancer. *Int J Mol Sci* 2017;18.
23. Klein CA, Seidl S, Petat-Dutter K, et al. Combined transcriptome and genome analysis of single micrometastatic cells. *Nat Biotechnol* 2002;20: 387–92.
24. Abrahamsen HN, Hamilton-Dutoit SJ, Larsen J, et al. Sentinel lymph nodes in malignant melanoma: extended histopathologic evaluation improves diagnostic precision. *Cancer* 2004;100: 1683–91.
25. Cochran AJ, Balda BR, Starz H, et al. The Augsburg consensus. Techniques of lymphatic mapping, sentinel lymphadenectomy, and completion lymphadenectomy in cutaneous malignancies. *Cancer* 2000;89:236–41.